Fabrication of Planar-Type Ti/TiO_x/Ti Junction by SPM Local Oxidation for a Resistive Switching Device

Rachsak Sakdanuphab[1] and Aparporn Sakulkalavek[2]
[1] College of Advanced Manufacturing Innovation, King Mongkut's Institute of Technology Ladkrabang
1 Chalongkrung Rd., Ladkrabang, Bangkok 10520, Thailand
[2] Department of Physics, Faculty of Science, King Mongkut's Institute of Technology Ladkrabang
1 Chalongkrung Rd., Ladkrabang, Bangkok 10520, Thailand
E-mail: [1]rachsak.sa@kmitl.ac.th, [2]aparporn.sa@kmitl.ac.th

Abstract: Metal/Insulator/Metal (MIM) junctions are promising to be a resistive random access memory (RRAM). Almost MIM junction has been fabricated by stack-multilayer depositions. In this work, we study the planar-type Ti/TiO_x/Ti junctions prepared by Ti sputtered film on SiO_2/Si wafer, following with photolithography process, and local anodic oxidation by scanning probe microscopy (SPM). The growth and characterization of TiO_x nanowires were investigated by atomic force microscopy (AFM). The oxide growth mechanism is proposed based on anodic oxidation theory. A resistive switching (RS) behavior of the junction was obtained by current-voltage measurement. Our results show the ability of SPM to growth TiO_x nanowires as an insulator and the junctions have a resistive switching ability that can switch from a high-resistance state (HRS) to a low-resistance state (LRS) and from LRS to HRS.

Keywords-- **RRAM, Scanning probe microscopy, Local anodic oxidation**

1. Introduction

Resistive random access memory (RRAM) is one of the most promising next generation nonvolatile memories (NVM) [1]. RRAM has attracted research attention due to their low power consumption, high speed operation, and excellent scalability [2,3]. Moreover, RRAM has a simpler cell structure compared with magnetic random access memory and ferroelectric random access memory. The cell structure, known as a resistive switching (RS) device, consists of metal/insulator/metal (MIM) junction that can change a resistance under the applied voltage or current. Normally, the applied voltage is used to control resistance states by set and reset voltages. The device can be switched from high-resistance state (HRS) to low-resistance state (LRS) by set voltage and from LRS to HRS by reset voltage. Recently, varieties of materials with high-k dielectric such as ZrO_2, ZnO, CuO, SnO_2, TiO_2, Al_2O_3, and HfO_x, have been studied [4-8]. The different materials show a various RS characteristics, including two switching types based on previous literatures; unipolar switching and bipolar switching. In addition, set and reset voltages, reversibility, and stability are different. Several models have been proposed to explain the origin of RS mechanism such as filament theory of bulk effect and interface effect [9,10].

Scanning Probe Microscopy (SPM) is a well known technique in surface characterization. Owing to their development of SPM, local oxidation nanolithography by atomic force microscope (AFM) has been interested for metal-oxide nanofabrication. The local oxidation reaction performed by a tip biased on a metal surface and then the surface is transformed to a metal-oxide. The mechanism of local oxidation process has been reported by Garcia [11]. The AFM tip provides an area defined by a combination of the probe-sample surface geometry and environmental humidity to form a water meniscus. This water meniscus acts as an electrolyte and spatially confines the oxidation of the metal surface or the reaction into metal oxide. The local electric field is larger than a critical electric field to break the water molecules to H^+ and OH^- ions (typical about 1 V/nm) in water meniscus. The reaction is performed in atomic scale on the metal surface. Several metals have been studied to generate metal oxide such as Ti, Ni, Al Cr etc [12-14]. Tsai fabricated gallium, zinc and nickel oxide nanodot for RRAM application using AFM local oxidation technique [15]. He found that the process can produce high-density gallium oxide nanodots for the construction of NVM. The lateral NiO nanobelt RRAM performs very low power operation. AFM local oxidation on Zn has shown exceptional performance in ZnO thin-film transistors.

Normally, RS devices are fabricated by thin film growth of top/bottom metal electrodes with a middle metal-oxide insulator. This structure is difficult to analyze the RS mechanism such as conducting path and interface phenomena because of its very thin layer. Using AFM local oxidation, this offers a great opportunity to study the switching mechanism. In this work, we adapt AFM nanolithography process to fabricate titanium oxide nanowires on a single RRAM cell. The extensive research in this area is aimed at fabricating nanoscale devices such as metal-oxide-semiconductor (MOS) transistors and NVM through the precise control of the local oxide growth by the AFM probe.

2. Experimental

Planar-type Ti/TiO_x/Ti junctions were fabricated on SiO_2/Si(100) substrate. Before that, the substrates were cleaned were cleaned by a solvent clean, a RCA clean, followed by a dionized water (DI) rinse, and blow dry with nitrogen gas. It is immediately loaded into the vacuum chamber to deposit Ti thin film . Ti films were deposited by DC magnetron sputtering from 3 inch Ti target (purity 99.995%). The sputtering power was used at 80 W with the Ar gas pressure at 4.0×10^{-3} mbar for one minute. The substrate bias was applied at 60V during the sputtering. With these parameters we have obtained the film thickness of 10 nm with a roughness of 0.015 nm.

Photolithography process was employed to create pattern for MIM junction. Following the steps of photolithography: substrate cleaning, resist coating, UV-exposure, development, HF etching (Ti etching), and resist removing. In each step, baking process was used at 90 °C. Figure 1(a) shows the photolithography mask using in this work. The lithography pattern consists of two contact pads with junction area for nanowire growth as seen in Fig. 1 (b).

A commercial AFM (Park systems model XE100) was used to perform local oxidation in contact mode AFM. A Si cantilever (NSC36 series, Mikromasch) having a diameter of approximately 200 nm with the angle <40° was perform the local oxidation. Local oxidation parameters were investigated on Ti surface by various conditions such as tip biased at -6, -8, and -10 V, tip scanning speed at 0.25 to 1 µm/sec and a constant applied force at 12.59 nN. The humidity was control in standard acoustic enclosure about 60 %RH. Figure 1(c) illustrates the local oxidation on junction area by tip biased AFM. After that, RS behaviors of MIM junctions were characterized by current-volatage measurement (Keithley 2410 high voltage SourceMeter, USA).

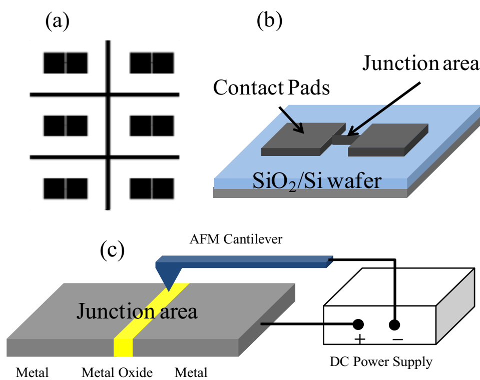

Figure 1. (a) Photolithography mask (b) Schematic diagram of RS device and (c) Illustration of the local oxidation on metal film by tip biased AFM.

3. Results and discussion

Normally, the oxidation mechanism and kinetics by SPM local oxidation are closely related to electrical field, surface stress, water meniscus formation, and OH^- diffusion. Figure 2 shows a mechanism of local oxidation on Ti surface based on the framework of Cabrera–Mott process [16]. It starts from an AFM probe approaching to a Ti surface, where a water meniscus is created around the tip-sample gap due to the capillary force. The water meniscus is dissociated by the negative tip biased, and the O^- and OH^- oxidative ions react with the substrate to form localized oxide nanostructures. The layer of absorbed water on the surface dissociates by a high electric field and acts as an electrolyte producing this electrochemical reaction. The chemical reactions and charge transfer processes can be considered as follows:

- Reactions at the Ti surface:

$$Ti + 2H_2O + 4h^+_{hole} \rightarrow TiO_2 + 4H^+$$

$$2H_2O + 4h^+_{hole} \rightarrow O_2\uparrow + 4H^+$$

- Reaction at an AFM probe:

$$4H_2O + 4e^- \rightarrow 2H_2\uparrow + 4OH^-$$

- Reaction in water:

$$4H^+ + 4OH^- \rightarrow 2H_2O$$

where, h^+_{hole} is a positively charged hole on the Ti surface. In addition, H_2 and O_2 gases from the reaction expose to environment. During the oxidation process, it is expected that the H^+ and OH^- ions generated at the Ti surface and an AFM probe will recombine immediately according to the recombination reaction in water and TiO_x.

TiO_x nanowires produced by various tip biased and tip scanning speed are presented in this section. A line pattern created by software is used to perform the local oxidation on various growth conditions. Fig. 3(a) shows the TiO_x nanowires performed by constant tip scanning speed at 0.5 µm/sec and tip biased at -6, -8, -10V from the left to the right hand side. The width of the wires is in the range of 40-170 nm by the increase of tip biased. At bias voltage below -6 V, the oxide height cannot observe. It may due to the low electric field to generate O^- and OH^- for oxidation reaction. This result shows that tip biased is very important for the oxide formation. The wire height increases with increasing tip voltage between 2.5-8.0 nm. It causes the enhanced decomposition exponentially under the larger tip biases as explained by R. García [12]. In addition, nanowires with critical dimension widths of less than 100 nm were fabricated with precisely.

The tip scanning speed is an important parameter to fabricated TiO_x nanowires by AFM local oxidation. Fig.3(b) depicts the nanowires performed by constant tip biased at -8V and use tip scanning speeds at 1, 0.75, 0.5, 0.25 µm/sec from the left to the right hand side, respectively. The width of TiO_x nanowire slightly increases in the range of 50-100 nm as a function of tip scanning speed while the wire height is nearly the same at 5.0 nm. This result shows the saturation of oxidation reaction with tip scanning speed.

Both parameters were optimized for creating a TiO_x nanowire on RS junction. The optimize condition was performed on the junction area by tip biased at -8V with tip scanning speed at 0.5µm/sec. The nanowire width and height are 120 nm and 4.0 nm, respectively. Figure 4 shows optical microscope image of junction area (a) and AFM image of the junction area (b). An arrow indicates TiO_x nanowires with the dimension of 120nm x 45µm. The design and the real device were not completely incorporated due to the photolithography process (wet etching). After that the RS devices were analyzed by measurement I-V characteristics.

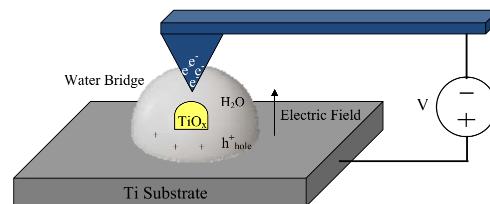

Figure 2. Schematic of TiO_x growth model by local anodic oxidation on thin Ti films based on the spatial confinement of a chemical reaction with a nanometer region.

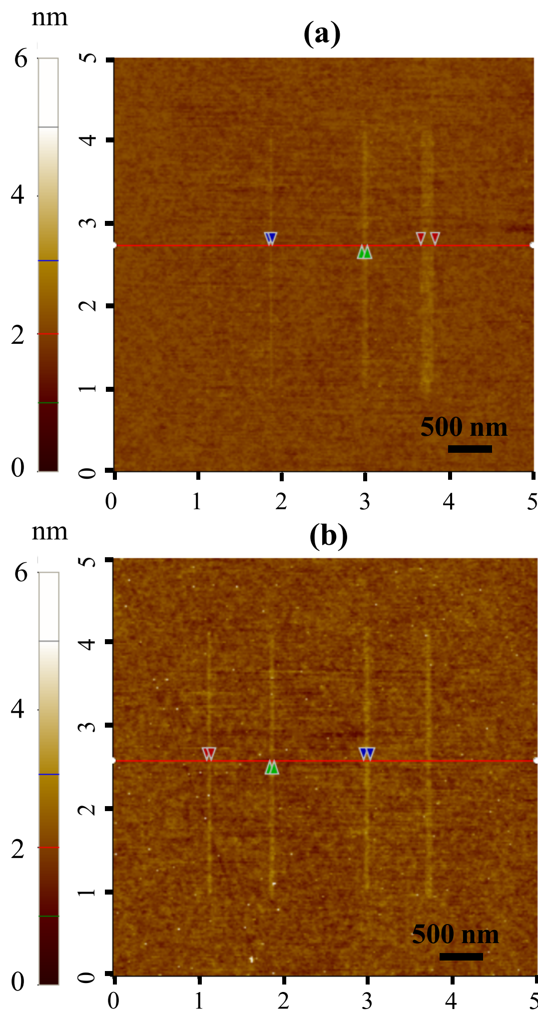

Figure 3. TiO_x nanowire (a) prepared by different tip biased at -6, -8, and -10V at scanning speed of 0.5 µm/sec, (b) prepared by different tip scanning speed at 1, 0.75, 0.5, and 0.25 µm/sec at tip biased at -8V from the left to the right hand side, respectively.

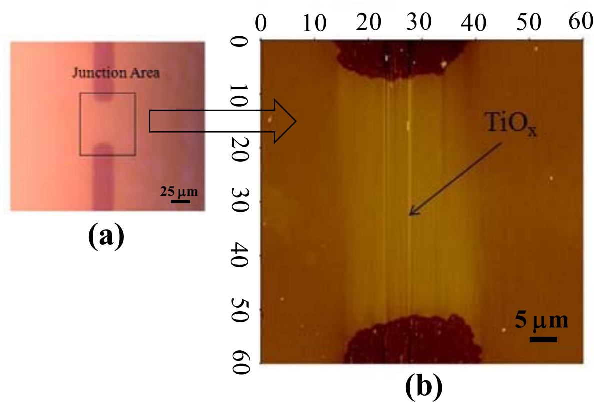

Figure 4. (a) Optical microscope and (b) AFM images of the junction area for RS device where TiO_x nanowire is indicated by an arrow.

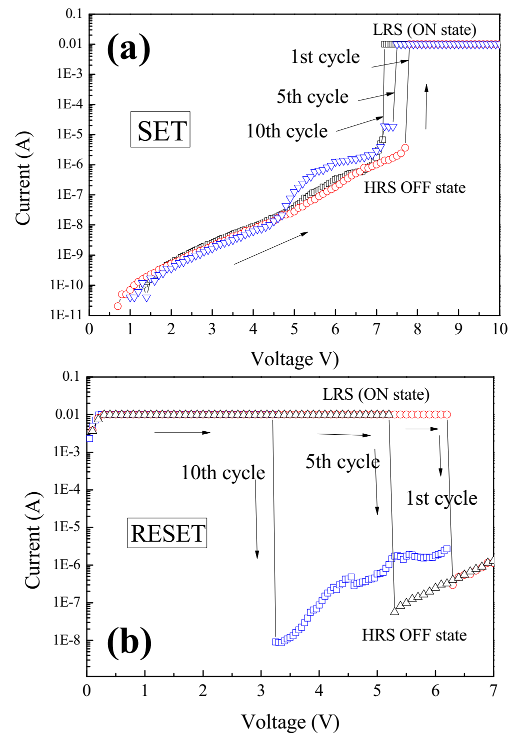

Figure 5. Cycle life, stability, and switching characteristics of the Ti/TiO_x/Ti obtained by I-V measurement (a) SET from HRS to LRS, and (b) RESET from LRS to HRS. Arrows indicate the sweeping directions.

The RS behaviors and memory efficiency of the planar Ti/TiO_x/Ti structure were studied by dc voltage sweep measurements. Figure 5(a), and 5(b) show the results of log plot I-V characteristics. The activation of the MIM structure device cells require a forming process with a forming voltage of about 8.0 V at applicable current compliance of 10 mA. The current compliance is limited in order to prevent the TiO_x nanowire from permanent breakdown. After the initial forming process, a steady increase of the positive voltages imposed on the device, an obvious change of resistance from the LRS (ON state) to the HRS (OFF state) is observed at about 6.4 V (1st cycle), this RS is called the ''reset'' process. The current of the device shows an opposite sharply decrease and nonvolatile switching is achieved for unipolar resistive switching. Subsequencly, the device cells are switched from the high resistance state (HRS) to the low resistance state (LRS) as seen the direction from arrows in Fig.5(a). The switching voltages at 1st , 50th and 100th cycles are 7.2, 7.5, and 7.6 V, respectively. The resistance ratio of HRS to LRS is as high as three orders of magnitude for the planar-type junction. The ''reset'' voltage (LRS to HRS) is decreased when sweeping the voltage to 5.4 and 3.2 V at 50th and 100th cycles. The result indicated that device cells show a degradation of reset state during the 100 repeated sweep cycles. From these measurement results, we conclude that the planar-type junction fabricated by AFM local oxidation are good controllable, reversible, and reproducible for nonvolatile memory application.

4. Conclusions

In conclusion, we achieve to fabricate planar-type Ti/TiO_x/Ti junctions by SPM local oxidation. The TiO_x formation can be explained by electrochemical reaction of Ti with O^- and OH^- oxidative ions supplied by water meniscus. Both tip biased and tip scanning speed are mainly important for TiO_x nanowire fabrication. In this study, the optimize condition is tip biased and tip scanning speed at -8V and 0.5 μm/sec, respectively. The planar-type junction exhibits unipolar resistive switching behavior with operating voltages (Set: 7.5 V and Reset: 5.4 V). The device cells are reversible RS characteristic within 100 cycles of the stability test. Planar-type Ti/TiO_x/Ti junctions is a good candidate for RRAM.

5. Acknowledgments

Author would like to acknowledge College of Advanced Manufacturing Innovation, King Mongkut's Institute of Technology Ladkrabang (KMITL). We would like to thank Department of Electronics, Faculty of Engineering, KMITL for allowing us to access their facility. In this work, the research was financial supported by Youth Fund Project of Development and Promotion of Science and Technology Talents (DPST Research Grant 029/2557). The author would like to acknowledge Dr. Siraphat Pratontep for discussion.

References

[1] G.I. Meijer, "Who wins the nonvolatile memory race?," *Science*, vol. 319, Issue 5870, pp.1625-1326, 2008.
[2] Y.C. Yang, "Fully room-temperature-fabricated nonvolatile resistive memory for ultrafast and high-density memory application," *Nano Lett.*, vol 9, Issue 4, pp.1636-1643, 2009.
[3] H.Y. Lee, "Low power and high speed bipolar switching with a thin reactive Ti buffer layer in robust based RRAM," *Tech. Dig. - Int. Electron. Dev. Meet.* (IEDM), pp.297-300, 2008.
[4] Y.S. Chen, "Highly scalable hafnium oxide memory with improvements of resistive distribution and read disturb immunity," *Tech. Dig. - Int. Electron. Dev. Meet.* (IEDM), pp.105-118, 2009.
[5] W.Y. Chang, "Unipolar resistive switching characteristics of ZnO thin films for nonvolatile memory application," *Appl. Phys. Lett.*, vol.92, Issue2, pp.022110.1-3.
[6] Q. Liu, "Improvement of resistive switching properties in ZrO_2-based ReRAM with implanted Ti ions," *IEEE Electron. Dev. Lett.*, vol.30, no.12, pp.1335-1337, 2009.
[7] W.H. Guan, "Nonpolar nonvolatile resistive switching in Cu doped ZrO_2," *IEEE Electron. Dev. Lett.*, vol.29, no.5, pp.434-437, 2008.
[8] C.H. Kim, "Observation of bistable resistance memory switching in CuO thin films," *Appl. Phys. Lett.*, vol.94, no. 10, pp. 102107.1-102107.3, 2009.
[9] M.C. Chen, "Influence of electrode material on the resistive memory switching property of indium gallium zinc oxide thin films," *Appl. Phys. Lett.*, vol.96, no.14, pp. 262110.1-262110.3, 2010.
[10] G. Dearnaley, "Electrical phenomena in amorphous oxide films," *Rep. Prog. Phys.*, vol.33, no.3, pp.1129-1191, 1970.
[11] J.J. Ahn, "Nano-structure fabrication of GaAs using AFM tip-induced local oxidation method: different doping types and plane orientations," *Nano. Res. Lett.*, vol.6, no. 550, pp.1-9, 2011.
[12] R. García, "Patterning of silicon surfaces with noncontact atomic force microscopy: field-induced formation of nanometer-size water bridges," *J. Appl. Phys.* vol. 86, issue 4, pp. 1898-1991, 1999.
[13] W.P. Huang, "Localized electrochemical oxidation of p-GaAs(100) using atomic force microscopy with a carbon nanotube probe," *Nanotechnology*, vol.17, no.15 pp.3838-3340, 2006.
[14] S.Y. Wang, "Improved resistive switching properties of Ti/ZrO_2/Pt memory devices for RRAM application," *Microelectron. Eng.*, vol. 88, Issue 7, pp.1682-1632, 2011.
[15] J.T.H. Tsai, "Rapid synthesis of gallium oxide resistive random access memory by atomic force microscopy local anodic oxidation," *Electron. Lett.*, vol.49, no. 8, pp.06527556-2, 2013.
[16] A.E. Gordon, "Mechanisms of surface anodization produced by scanning probe microscopes," *J. Vac. Sci. Technol. B*, vol.13, Issue 6, pp.2805-2808, 1995.